ISSN : 0974 - 746X Volume 8 Issue 4

Inorganic CHEMISTRY

An Indian Journal

Full Paper

ICAIJ, 8(4), 2013 [116-122]

Structural comparative studies on new Pt^{IV} complex derived from 2,4,6-tri-(2-pyridyl)-1,3,5-triazine (TPTZ)

W.H.Al-Assy, A.H.El-Askalany, M.M.Mostafa*

Chemistry Department, Faculty of Science, Mansoura University, (EGYPT)

E-mail : amohsenmostafa@yahoo.com

ABSTRACT

The structure of a new Pt^{IV} complex, $[Pt_3^{IV}(TPTZ)Cl_8].2H_2O.4Cl$, was established and characterized by elemental analyses, spectral, magnetic, thermal and cyclic voltammetry measurements. Electronic spectra of the complex suggest distorted-octahedral structures around the Pt^{IV} ion. The HOMO, LUMO and other DFT parameters on the atoms have been calculated to confirm the geometry of the ligand and the complexes using material studio program. The redox properties were investigated by cyclic voltammetry. Kinetic parameters were determined using Coats-Redfern and Horowitz-Metzger methods. The results of biological activity for the Pt^{IV} complexes promised to be effective in tumour treatment.

KEYWORDS

Structural comparative studies on new Pt^{IV} complex; IR and ^{1}H-NMR studies; DNA studies.

INTRODUCTION

2,4,6-Tri-(2-pyridyl)-1,3,5-triazine (TPTZ) has been used as analytical reagent for various metal ions[1-6], as a spacer for designing supramolecular complexes[7-12] and for synthesis of transition metal complexes[13-20]. In recent years, an explosion of interest in the platinum terpy family of complexes, It is widely acknowledged that DNA is the major target of platinum based antitumor chemotherapy antitumor drug and widely used to treat various types of human cancer[21]. In this paper we report the isolation and characterization of a new Pt^{IV} complex using elemental analyses, spectral (UV-Vis., ^{1}H-NMR and FTIR), magnetic, thermal (TGA), cyclic voltammetry (CV) and DFT measurements. In a tridentate and bidentate manner three independent Pt^{IV} ions coordinated with two TPTZ ligands so it appears as trinuclear complex and formed complete a distorted-octahedral geometry around the three Pt^{IV} ions.

EXPERIMENTAL

2,4,6-Tri-(2-pyridyl)-1,3,5-triazine (TPTZ) was purchased from BDH and used without purification. All the solvents and $PtCl_4$ were of BDH quality and used without purification.

Synthesis of Pt^{IV} complex

The ligand (2,4,6-tri-(2-pyridyl)-1,3,5-triazine; 1 mmol) was dissolved in a solution of THF and EtOH (3:1) and added to $PtCl_4$ solutions in THF and EtOH (1 mmol; 3:1). The reaction mixture was refluxed on a hot plate for 2 h. The complex was isolated in the pH 5-6 range and the product was filtered off, washed several times with hot EtOH, dried in an oven at 120 oC for 0.5 h and finally kept in a desiccator over P_4O_{10}.

The chemical formula of the orange Pt^{IV} complex, $[Pt_3^{IV}(TPTZ)Cl_8].2H_2O.4Cl$, was suggested on the basis of elemental analyses (Found: C, 26.36; H, 2.35; Pt, 35.59; Cl, 24.6%. Calcd.: for $C_{36}H_{28}Cl_{12}Pt_3N_6O_2$: C, 25.9; H, 1.7; Pt, 35; Cl, 25.7%), m.p.; > 300 °C; Yield: 69.4%).

Physical measurement

Carbon and hydrogen contents were performed at the Micro-analytical Unit at Cairo University. Metal and chloride contents were determined by the standard methods[22]. Cyclic voltammetric studies were carried out on electroanalyzer CHI 610A, the three electrode cell comprised a reference Ag wire, Pt auxiliary and Pt electrode. $[(n\text{-}Bu)_4N]PF_6$ (0.1 M) was used as electrolyte and add to the complex (10^{-3} M). The calculations of modeling have been carried out using Gaussian energy calculation DFT. The DFT calculations were performed with the use of B3LYP/LanL2MB hybrid functional as implemented by materials studio[23-25]. All spectral (IR and UV-Vis) measurements were made as reported earlier[19].

RESULTS AND DISCUSSION

TPTZ coordinates with the metal ions in different modes as reported earlier[5]. TPTZ forms different kinds of mononuclear, binuclear and trinuclear complexes.

IR spectrum of TPTZ

The IR spectrum of TPTZ shows six bands at 1673, 1620, 1586, 1529, 1469, and 1436 cm^{-1}. The first four bands are assigned to (C=N) (triazine, free), (C=N) (triazine, hydrogen-bonded), (C=N+C=C) (Py, free), (C=N+C=C) (Py, hydrogen-bonded). The latter two bands are attributed to ν[(C-N)+(C-C)], respectively. The spectrum also shows two strong bands at 3382 and 3259 cm^{-1} assigned to $\nu_{as}(H_2O)$ and $\nu_s(H_2O)$ vibrations. These bands are mainly due to the contamination of KBr with small amounts of H_2O. The existence of water within the ligand forms external hydrogen bonding between C=N of TPTZ and OH (H_2O). Weak broad bands at 2173 cm^{-1} confirm the existence of hydrogen bonding of the type O–H…N. But in Nujol mull the ligand shows four bands due to the C=N (triazine and Py) and C=C vibrations at 1652, 1586, 1529, and 1464 cm^{-1}. The C=N bands are observed at higher wave-numbers. The shifts indicate the partial destruction of hydrogen bonding between C=N and OH. The C=C vibrations remain more or less at the same positions indicating that they do not participate in hydrogen bonding. The decrease of intensity of the OH bands and the observation of new bands at 3363 and 3244 cm^{-1} suggests that the hydrogen bonding is weak, but still exists within the ligand as shown in Figure 1. On comparing the IR spectra of the ligand in KBr and Nujol with the Pt^{IV} complex the results show a broad band at 3442 and 3426 cm^{-1} assigned to the water molecules (O-H stretching) and a shoulder at 1646 cm^{-1} assigned to the H-O-H bending mode). The bands characteristic of TPTZ in the complex appear at 3068 cm^{-1} with a shoulder at 3100 cm^{-1} assigned to the aromatic C–H stretching vibrations. Also, the bands at 1614, 1579 and 1527 cm^{-1} are attributed to ν[C= N+CC] vibrations. The bands observed in the 1481-1241 region are assigned to the ν[(C-N)+C-C] vibrations while the band at 771 cm^{-1} is assigned to the aromatic C-H deformation vibrations[26-28]. Also, our previous results confirm that the mode of bonding of TPTZ with Pt^{IV} ions is quite similar[21].

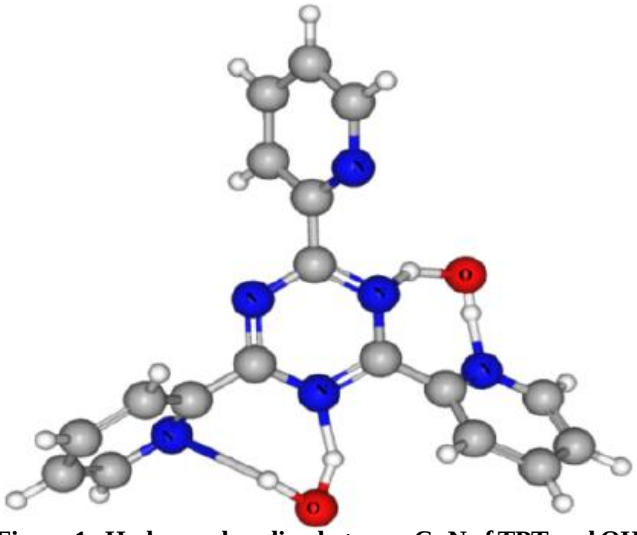

Figure 1 : Hydrogen bonding between C=N of TPT and OH (H_2O)

^{1}H-NMR spectrum of TPTZ

The ^{1}H-NMR spectrum of TPTZ in d_6-DMSO shows four signals assigned for 12 aromatic protons as expected for three magnetically equivalent pyridyl rings. Each ring of the three pyridyl contains the same type of

Full Paper

protons. Also, the spectrum shows four signals (Supplementary material) with equal intensity at δ = 7.72 (ddd, 3H), 8.13 (td, 3H), 8.75 (d, 3H), and 8.91 (d, 3H) ppm which are assigned to H_5, H_4, H_3 and H_6, respectively, with respect to TMS as shown in Figure 2.

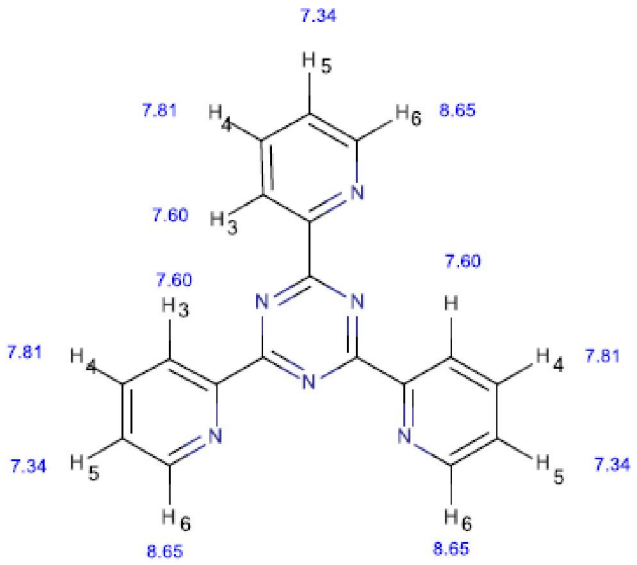

Figure 2 : Signals (δ) of different protons of TPTZ

Electronic spectra of Pt^{IV} complex

Pt^{IV} complex usually shows intense peaks in the UV region corresponding to ligand-based π→π* transitions with overlapping metal-to-ligand charge-transfer (MLCT) in the visible region. The electronic spectrum of the tri-nuclear Pt^{VI} complex was recorded in Nujol. The geometry of the octahedral Pt^{VI} suggests a low-spin configuration with $(t_{2g})^6$ and show high intensity bands at low energy region around (312–600 nm) refers to the d-d transition bands $^1A_{1\rightarrow}\ ^1T_2$, $^1A_{1\rightarrow}\ ^1T_1$, $^1A_{1\rightarrow}\ ^3T_2$, A and $^1A_{1\rightarrow}\ ^3T_1$. But the bands at 470 and 600 nm are characteristic of the metal ligand charge-transfer (MLCT), Pt(dπ)→L(π*) transitions involving the various pyridyl components of the coordinated ligands, respectively.

^{1}H-NMR of of Pt^{IV} complex

The ^{1}H-NMR spectrum of the Pt^{IV} complex was recorded in d_6-DMSO. The position and integrated intensity of the various signals corresponding to TPTZ corroborated well to a system involving coordination of TPTZ with Pt^{IV} ion expected for the six magnetically equivalent coordinated pyridyl rings as mode of chelation (VII) in (Figure 3). However, only four distinct signals are observed in the Pt^{IV} complex. The ^{1}H-NMR spectrum of the Pt^{IV} complex displays overlapping signals at δ = 9.02 (d, 6H), 8.93 (d, 6H), 8.3(t, 6H), and 7.9(t, 6H) ppm are assigned to H6-62 , H3-32 , H4-42 and H5-52 , respectively, with respect to TMS. The signal at δ = 3.8 ppm in the Pt^{IV} complex is assigned to the protons of the coordinated H_2O which appear as a broad sharp signal referring to the existence of H_2O molecules. After comparing this data with the ligand all the protons have shifted to downfield confirming the coordination of the ligand to the Pt^{IV} ion.

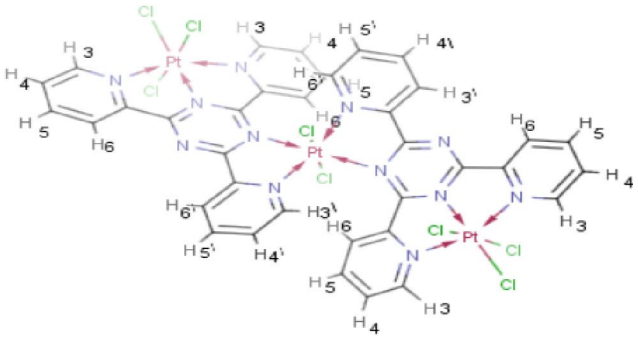

Figure 3 : Different protons of $[Pt_3^{IV}(TPTZ)Cl_8].2H_2O.4Cl$

Thermal measurements of Pt^{IV} complex

The TGA of the Pt^{IV} complex (under nitrogen) was carried out in the range 40–1000 °C to insight about their thermal stability. The data showed that the water of crystallization are volatilized at 62 °C[29]. The TGA curve of the $[Pt_3^{IV}(TPTZ)Cl_8].2H_2O.4Cl$ shows a first step in range 40-163 °C with gradual mass loss corresponding to two water molecules (lattice) 2.2% (2.16). The second step is observed in the range 164-324 °C with gradual mass loss corresponding to six chlorine ions 11.7% (12.7). The mass loss corresponds to the ligand of the main skeleton for the complex and six chlorine ions are 48.9% (48.0%) in range 315-718 °C. The experimental residual part 37 %(37.2 %) refers to 3PtC. The total loss is 63.0%. It is clear that, the TG curve for the investigated complex displays high decomposition part in range over 324 °C to 805 °C indicating the high stability of this complex.

Molecular modelling and DFT calculations

All DFT calculations were performed cluster calculations using $DMOL^3$ program[23] in Materials Studio package[24], which is designed for the realization of large scale density functional theory (DFT) calculations. DFT

semi-core pseudopods calculations (dspp) were performed with the double numeric basis sets plus polarization functional (DNP). The DNP basis sets are of comparable quality to 6-31G Gaussian basis sets[25]. The molecular structure along with atom numbering of the Pt^{IV} complex is shown in Figures 4-8. The structure of complex consists of the cationic complex $[Pt_3^{IV}(TPTZ)Cl_8]^{+4}$ and a four chlorine as counter ion. In this complex, there are three independent Pt^{IV} ions coordinated with two TPTZ ligands so it appears as trinuclear complex. Two of this ions [Pt(49) - Pt(51)] have same coordination by one triazine and two pyridine nitrogen atoms of two TPTZ ligand but the other Pt^{IV} ion [Pt(50)] is coordinated as a bridge between the two TPTZ through one triazine and one pyridine rings of each of them. The coordination sphere around Pt(49) and Pt(51) has a distorted-octahedral geometry but around Pt(50) a high distortion is observed from the difference of bond angels and bond length. The distortion around the Pt^{IV} ion is due to the rigidity of the donor environment of TPTZ. The coordination sphere around Pt(49) through the atoms N(4) of triazine, N(18) and N(10) of pyridine rings with one of chlorine ion Cl(55) in equatorial position and other two chlorine Cl(56)- Cl(57) ions in axial position. Also, the results indicate that all the bond distances and angles around the Pt(49) ion are quite different in which the chelating angles N4-Pt49-N18 [79.37°], N4-Pt49-N10 [79.04°], N10-Pt49-Cl55 [100.84°] and N18-Pt49-Cl55 [100.75°] are less or larger than ideal value (90°) and the Cl56- Pt49-Cl57 bond angle [178.9°] near from ideal value (180°) but N4-Pt49-N18 [158.4°] is less than that observed for Pt49-Cl and the bond lengths are approximately equal [2.369Å and 2.373Å]. The Pt49-N (pyridyl) bonds [2.111and 2.113 Å] tend to be slightly longer than the Pt49-N(triazine) bond [1.99 Å]. Similarly Pt(51) which has same block coordination position has quite different bond distances and angles. In which the chelating angles N34-Pt51-N28 [79.07°], N42- Pt51-N28[79.36°], N34- Pt51-Cl52 [100.85°] and N42- Pt51-Cl52 [100.71°] are less or larger than ideal value of 90° and the Cl54- Pt51-Cl53 bond angle [179°] near from ideal value (180°) but N34-Pt51-N42 [158.4²°] but are less than it and the Pt51-Cl bond lengths are approximately equal [2.369, 2.372 and 2.351 Å]. The Pt51-N (pyridyl) bonds [2.112 and

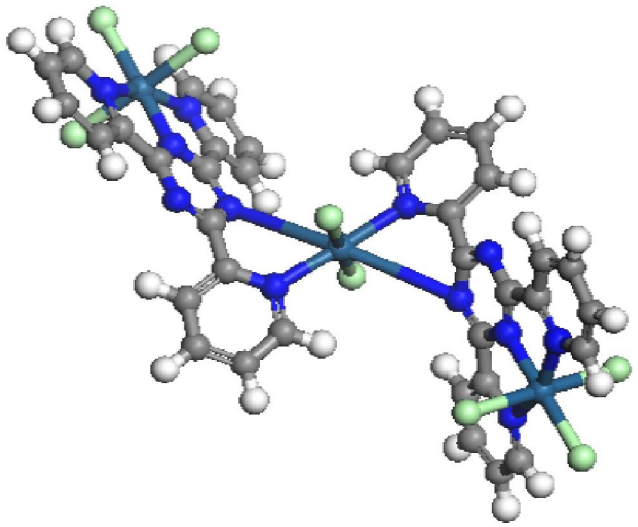

Figure 4 : Molecular modeling of $[Pt_3^{IV}(TPTZ)Cl_8].2H_2O.4Cl$

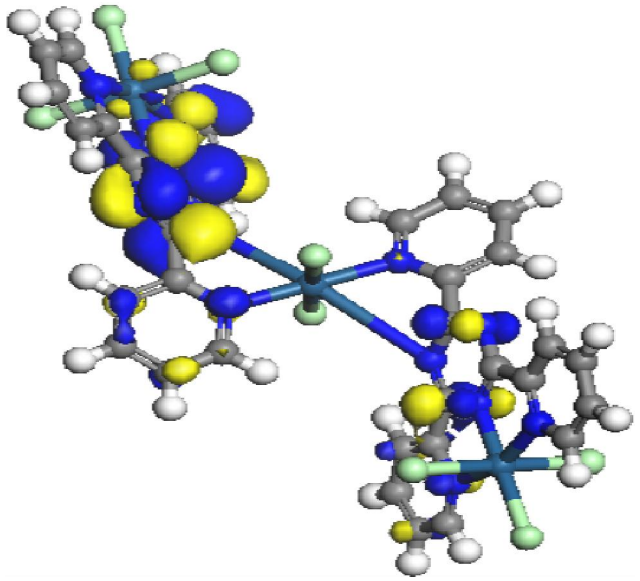

Figure 5 : LUMO of $[Pt_3^{IV}(TPTZ)Cl_8].2H_2O.4Cl$

2.108 Å] tend to be slightly longer than the Pt51-N(triazine) bond [1.99 Å]. Each of Pt(51) and Pt(49) ions with its triazine and pyridine coordination rings found in coplanar plane. In case of Pt(50) have high deviation in its geometry and this due two twisted an deviation of the two pyridyl rings of two TPTZ from the planarity of its ligand in addition to the high rigidity of the two triazine rings in two TPTZ so that the Pt(50) and chelation rings not found together as a coplanar. The pyridyl(N47) ring twisted by dihedral angle [44.25°] along $C_{triazine}$–$C_{pyridine}$ (C25-C43) bond and deviation by angle [14°] but The pyridyl (N23) ring twisted by dihedral angle [47.07°] along $C_{triazine}$–$C_{pyridine}$ (C1-C19) bond and deviation by angle [15.74°]. The chelating angles

Full Paper

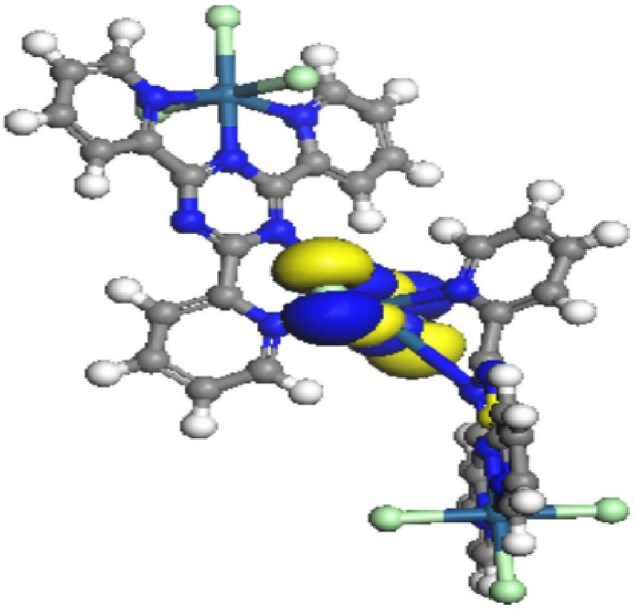

Figure 6 : HOMO of $[Pt_3^{IV}(TPTZ)Cl_8].2H_2O.4Cl$

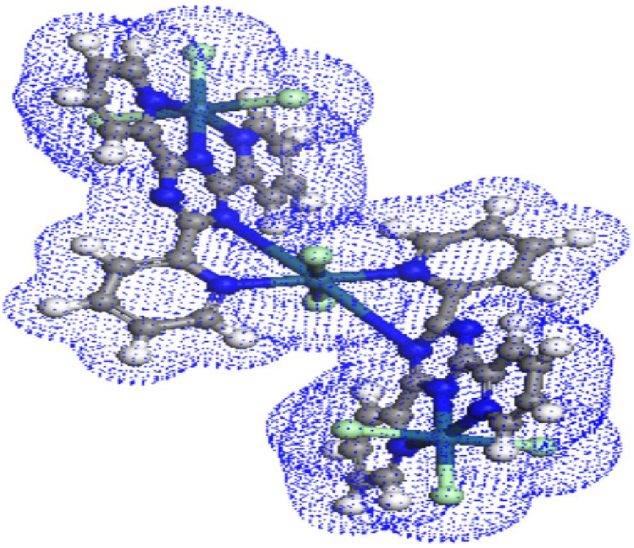

Figure 7 : Electron density of $[Pt_3^{IV}(TPTZ)Cl_8].2H_2O.4Cl$

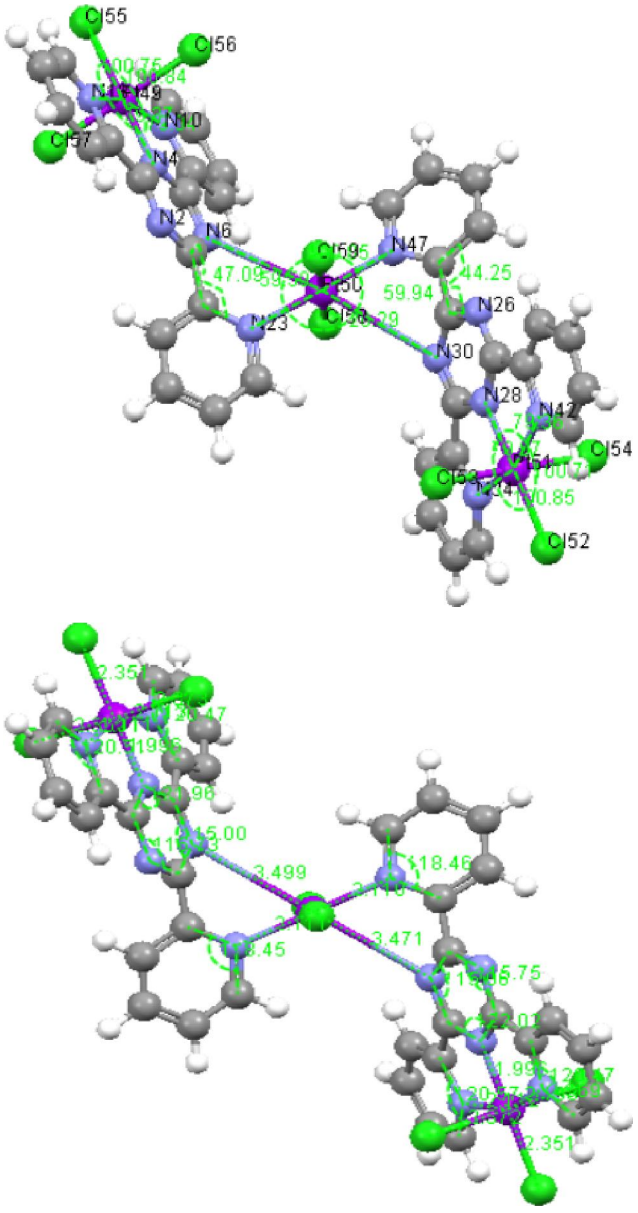

Figure 8 : Tetrahedral and different angles of $[Pt_3^{IV}(TPTZ)Cl_8].2H_2O.4Cl$.3. 7. kinetic data

N47-Pt50-N30 [59.59°], N6- Pt50-N23 [59.94°], N30- Pt50-Cl23 [120.28°] and N47- Pt50-Cl6 [120.85°] are less or larger than ideal value of 90° and the Cl58- Pt50-Cl59 bond angle [179.96°] like ideal value 180° but N6- Pt50-N30 [163°] less than it. The Pt50-Cl bond lengths are approximately equal [2.3Å] but the Pt50-N bonds are different where Pt50-N6 [2.5 Å], Pt50-N30 [2.47 Å], Pt50-N47 [2.110 Å] and Pt50-N23 [2.111Å]. The results show that the internal C-N-C angels of triazine in the Pt^{IV} complex are smaller than 120° for the two angles C27-N26-C25 [115.75°] and C25-N30-C29 [115.06°] while the third angle C27-N28-C29 [122.02] is larger than 120° but N-C-N is greater than120° like in ligand crystal [30, 31], and this for first triazine similarly second triazine has two angle C1-N6-C5 [115°] and C1-N2-C3 [115.73°] and the third angle C5-N4-C3[121.96] is larger than 120°. All C-N-C angles of the pyridyl rings are greater than that of free ligand [114.3°] where this angles pyridyl-N42 [120.47°], pyridyl-N34 [120.57°], pyridyl-N23 [118.45°], pyridyl-N47 [118.46°], pyridyl-N10 [115.73°] and pyridyl-N18 [115°]. This deviation of angle is due to high rigidity of ligand during the chelation with metal ions.

The kinetic and thermodynamic parameters of ther-

mal degradation process have been calculated using Coats–Redfern and Horowitz–Metzger models[32,33]. A number of pyrolysis processes can be represented as a first order reaction. Particularly, the degradation of a series of TPTZ complexes was suggested to be first order[34], therefore, we assume n=1 for the remainder of the present text. The other thermodynamic parameters of activation can be calculated by Eyring equation[35-36]. Thermodynamic parameters of decomposition steps were calculated using Coats–Redfern[32] and Horowitz–Metzger[33] methods. In both methods, the Ln [-Ln (1-α)] values are plotted against 1/T and θ ((T-Ts). The negative values of the entropy of activation (ΔS*) of the decomposition steps of the Pt^{IV} complex indicate that the activated fragments have more ordered structure than the un-decomposed complex and/or the decomposition reactions are slow[36]. The positive sign of ΔH* of the decomposition stages reveals that the decomposition stages are endothermic processes. Also, the positive sign of ΔG*, indicates that

TABLE 1 : Kinetic parameters evaluated by Coats-Redfern equation for TPTZ complex

Complex	Peak	Mid Temp(K)	Ea KJ/mol	A (S^{-1})	ΔH* KJ/mol	ΔS* KJ/mol.K	ΔG* KJ/mol
	1st	361	30.47	0.0503	27.469	-271.35	125.428
$[Pt_3(TPTZ)Cl_8].2H_2O.4Cl$	2nd	545	69.447	0.018 $X10^3$	64.916	-225.726	187.937
	3rd	878	51.455	0.00138	44.155	-308.622	315.126

TABLE 2 : Kinetic parameters evaluated by Horowitz-Metzger equation for TPTZ complex

Complex	Peak	Mid (K)	Ea KJ/mol	A (S-1)	ΔH*KJ/mol	ΔS*KJ/mol.K	ΔG*KJ/mol
	1st	361	33.426	$0.174X10^3$	30.424	-203.623	103.93
$[Pt_3(TPTZ)Cl_8].2H_2O.4Cl$	2nd	545	86.431	$8.272X10^6$	91.34	-117.499	155.38
	3rd	878	75.628	$0.048X10^3$	68.328	-221.692	262.97

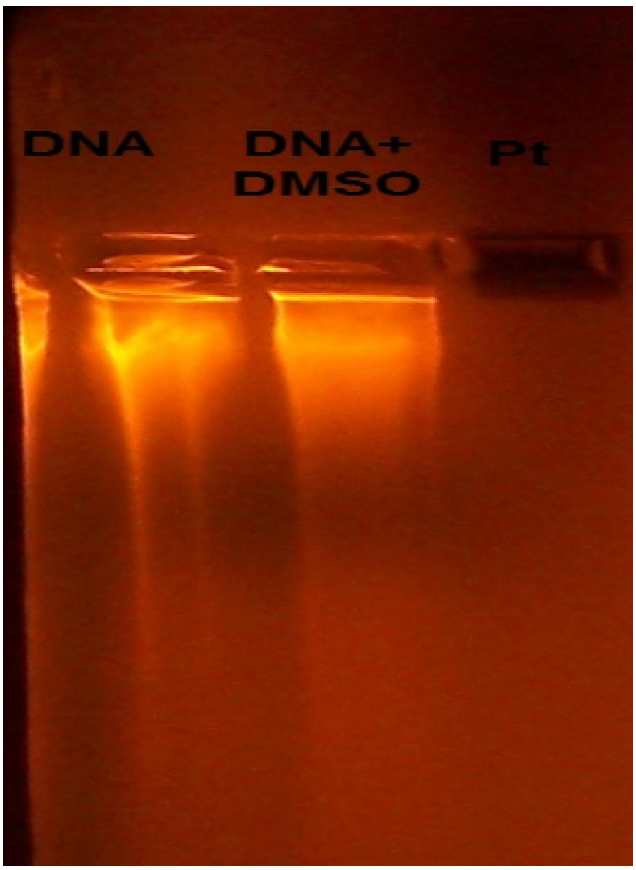

Figure 9 : The degradation power of the tested complex on Calf-Thymus DNA

the free energy of the final residue is higher than that of the initial compound and hence all the decomposition steps are nonspontaneous processes. Moreover, the values of ΔG* increase significantly for the next stages for a given compound. This reflects that the rate of removal of the subsequent species is lower than that of the precedent one[37-39]. This may be attributed to the structural rigidity of the remaining complex after the expulsion of one or more ligands, as compared with the precedent complex, which requires more energy, TΔS*, for its rearrangement before undergoing any decomposition change. Accordingly the values of the total activation energy, the thermal stability of the metal complexes with TPTZ is high[40].

CONCLUSION

In this work, the coordination chemistry of TPTZ and its Pt(IV) ion was investigated. The ligand coordinated to the Pt^{IV} ions in a tridentate manner with two pyridine N and triazine N donor sites. Additionally Pt(IV) complex possess high degradation power against Calf-Thymus DNA. Also, the geometry of the Pt(IV) complex is suggested by DFT calculation.

Full Paper

REFERENCES

[1] P.Collins, H.Diehl, G.F.Smith; Anal.Chem., **31**, 1862-1867 **(1959)**.
[2] P.Collins, H.Diehl; Anal.Chim.Acta., **22**, 125-127 **(1960)**.
[3] H.Diehl, E.B.Buchanan, G.F.Smith; Anal.Chem., **33**, 1117-1119 **(1960)**.
[4] C.C.Tsen; Anal.Chem., **33**, 849-851 **(1960)**.
[5] B.Therrien; J.Organometal.Chem., **696**, 637-651 **(2011)**.
[6] H.D.Arman, P.Poplaukhin, E.R.T.Tiekink; Acta.Cryst., E, **68**, 319-320 **(2012)**.
[7] H.Hadadzadeh, M.Maghami, J.Simpson, A.Khalaji, K.Abdi; J.Chem.Cryst., **42**, 656-667 **(2012)**.
[8] K.Abdi, H.Hadadzadeh, M.Salimi, J.Simpson, A.D.Khalaji; Polyhedron, **44**, 101-112 **(2012)**.
[9] Z.Ahmed, K.Iftikhar; Inorg.Chem.Commun., **13**, 1253-1258 **(2010)**.
[10] K.Ha; Acta.Cryst., E, **66**, m262 **(2010)**.
[11] M.M.Najafpour, M.Holynska, M.Amini, S.H.Kazemi, T.Lis, M.Bagherzadeh; Polyhedron, **29**, 2837-2843 **(2010)**.
[12] Z.Xiao, L.Wang, X.Zhao, X.Jiang, Z.Li; Tetrahedron Lett., **52**, 3836-3839 **(2011)**.
[13] J.Luo, L.Qiu, B.Liu, X.Zhang, F.Yang, L.Cui; Chinese J.Chem., **30**, 522-528 **(2012)**.
[14] W.A.Embry, G.H.Ayres; Anal.Chem., **40**, 1499-1501 **(1968)**.
[15] M.J.Janmohamed, G.H.Ayres; Anal.Chem., **44**, 2263-2268 **(1972)**.
[16] A.Gelling, M.D.Olsen, K.G.Orrell, V.J.Sik; Chem.Soc.Chem.Commun., 587-595 **(1997)**.
[17] E.Lerner, S.J.Lippard; J.Am.Chem.Soc., **98**, 5397-5398 **(1976)**.
[18] G.Y.S.Chan, G.B.Drew, M.J.Hudson, N.S.Isaac, P.Byers, C.Madic; Polyhedron, **15**, 3385-3398 **(1996)**.
[19] S.M.Al-Ashqar, M.M.Mostafa; J.Coord.Chem., **63**, 721-729 **(2010)**.
[20] K.Ha; Acta.Cryst., E, **67**, m1306 **(2010)**.
[21] S.Rubino, P.Portanova, A.Girasolo, G.Calvaruso, S.Orecchio, G.C.Stocco; Eur.J.Medic.Chem., **44**, 1041-1048 **(2009)**.
[22] A.I.Vogel; Text Book of Quantitative Inorganic Analysis, 3rd Edition., Longman, London, **(1961)**.
[23] **(a)** B.Delley; J.Chem.Phys., **113**, 7756-7764 **(2000)**; **(b)** X.Wu, A.K.Ray; Phys.Rev., **65B**, 85403-85409 **(2002)**; **(c)** B.Delley; Int.J.Chem., **69**, 423-433 **(1998)**.
[24] P.V.R.Schleyer, J.A.Pople, P.V.R.Schleyer, J.A.Pople; Initio Ab Initio Molecular Orbital Theory, John Wiley, New York, **(1986)**.
[25] A.atveev, M.Staufer, M.Mayer, N.RçSch; Int. J.Quantum Chem., **75**, 863-873 **(1999)**.
[26] M.M.Najafpour, M.Holynska, M.Amini, S.H.Kazemi, T.Lis, M.Bagherzadeh; Polyhedron, **29**, 2837-2843 **(2010)**.
[27] Z.Ahmed, K.Iftikhar; Inorg.Chem.Commun., **13**, 1253-1258 **(2010)**.
[28] A.Das, G.M.Rosair, M.S.J.El Fallah, R.S.Mitra; Inorg.Chem., **45**, 3301-3306 **(2006)**.
[29] M.Xing Li, Z.Xin Miao, M.Shao, S.Wen Liang, S.Rong; Zhu.Inorg.Chem., **47**, 4481-4489 **(2008)**.
[30] J.Janczak, M.Sledz, R.Kubiak; J.Mol.Struc., **659**, 71-79 **(2003)**.
[31] W.K.Pogozelski, T.D.Tullius; Chem.Rev., **98**, 1089-1108 **(1998)**.
[32] A.W.Coats, J.P.Redfern; Nature, **201**, 68-69 **(1964)**.
[33] H.H.Horowitz, G.Metzger; Anal.Chem., **25**, 1464-1468 **(1963)**.
[34] A.Broido; J.Polym.Sci.A-2: Poly.Phys., **7(10)**, 1761-1773 **(1969)**.
[35] A.A.Frost, R.G.Pearson; Kinetics and Mechanism, John Wiley, New York, **(1961)**.
[36] R.G.Mortimer; Physical Chemistry, Harcourt and Science Technology Company, Academic Press., San Diego, **(2000)**.
[37] P.B.Maravalli, T.R.Goudar, Thermochim.Acta., **325**, 35-41 **(1999)**.
[38] K.K.M.Yusuff, R.Sreekala; Thermochim.Acta., **159**, 357-368 **(1990)**.
[39] S.S.Kandil, G.B.El-Hefnawy, E.A.Baker; Thermochim.Acta, **414**, 105-113 **(2004)**.
[40] T.Hatakeyama, F.X.Quinn; Thermal Analysis Fundamentals and Applications to Polymer Science, 2nd Edition. John Wiley, Chichester, **(1994)**.
[41] U.El-Ayaan, M.M.Youssef, S.Al-Shihry; J.Mol.Struct., **936**, 213-219 **(2009)**.